

Supplementary material for "Impurity-induced magnetic order in low dimensional spin gapped materials"

J. Bobroff,¹ N. Laflorencie,¹ L. K. Alexander,¹ A. V. Mahajan,² B. Koteswararao,² and P. Mendels¹

¹*Laboratoire de Physique des Solides, Université Paris-Sud, UMR-8502 CNRS, 91405 Orsay, France*

²*Department of Physics, Indian Institute of Technology Bombay, Mumbai 400076, India*

In this supplementary material, we investigate further the impurity-induced freezing mechanism in a doped system of 3D weakly coupled ladders resembling $\text{Bi}(\text{Cu}_{1-x}\text{Zn}_x)_2\text{ZnPO}_6$ using QMC.

I. INTRODUCTION

In the previous letter [1], we have argued that the collective freezing of effective moments having a 3D extension $V_\xi \sim \xi_x \xi_y \xi_z$ at $T > T_g$ is actually controlled by the exponentially decaying 3D coupling of the general form

$$|J_{3D}^{\text{eff}}(\vec{r})| \simeq J_{3D} \exp\left(-\frac{x}{\xi_x} - \frac{y}{\xi_y} - \frac{z}{\xi_z}\right), \quad (1)$$

expected to occur for the wide class of spin gapped materials [2, 3, 4, 5, 6, 7]. The average coupling J_{avg} taken over all possible $J_{3D}^{\text{eff}}(\vec{r})$ does account for the broad distribution of effective interactions and is just given by

$$J_{\text{avg}} = \langle |J_{3D}^{\text{eff}}(\vec{r})| \rangle \simeq J_{3D} \frac{xV_\xi}{1 + xV_\xi} \quad (2)$$

where $V_\xi \sim \xi_x \xi_y \xi_z$ is the magnetic volume occupied by each induced moment. We propose that this average coupling governs the ordering, i.e. $T_g \simeq J_{\text{avg}}$.

II. MICROSCOPIC MODEL

We want to check such an analysis against QMC simulations on a diluted 3D model of weakly coupled ladders (schematized in Fig. 1) with the following parameters: $J_\perp/J = 0.1$ and $J_{3D}/J = 0.05$ which, using a value of $J \simeq 100$ K corresponds to a spin gap $\Delta \simeq 35$ K and a transverse 3D coupling $J_{3D} \simeq 5$ K. We then introduced non-magnetic impurities (open circles in Fig. 1) and performed large scale QMC simulations on 3D samples of sizes $L \times L \times L/2$, with $L = 16, 24, 32, 48$, down to temperature $T/J = 0.01$. We also performed disorder averaging over a large number N of independent disordered samples ranging from $N = 500$ for $L = 16$ to $N = 100$ for $L = 48$.

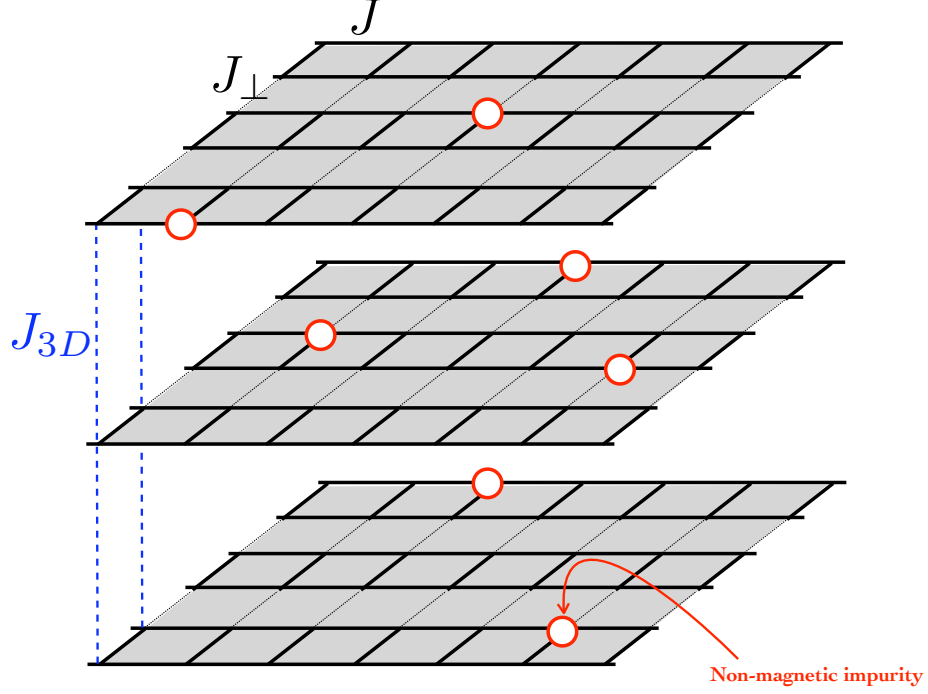


FIG. 1: (Color online) Schematic picture of the 3D system of coupled ladders used for the QMC simulations.

III. QMC RESULTS FOR THE CRITICAL TEMPERATURE

The results for the 3D ordering temperature T_g are shown in Fig. 2 versus the impurity concentration x . The transition was found by the standard technique using the finite size scaling of the spin stiffness at the transition point, as exemplified in Fig. 3 and discussed below. As shown in Fig. 2, we get a linear increase for $T_g(x)$ up to a threshold $\sim 3\%$ where T_g saturates as expected. The linear part can be fitted by the form $T_g = 2.8x$ which compares quite well to our estimate Eq. (2). Indeed, with our parameters, we expect an average coupling $J_{\text{avg}} \approx J_{3D} \times V_\xi \times x \approx 0.05 \times 30 \times x = 1.5x$, meaning that with such a definition for V_ξ , we get $T_g(x) \approx 2J_{\text{avg}}$.

IV. DETAILS ABOUT THE CRITICAL POINT

The way the critical ordering temperature was extracted from QMC simulations on finite size systems is actually standard since it relies on the finite size scaling of the order parameters, as for instance used in Ref. [8]. Therefore we computed the spin stiffness ρ_s , directly related to the square of the AF order parameter. In an 3D AF ordered phase ρ_s is finite whereas it is 0 in a disordered phase. At the critical point

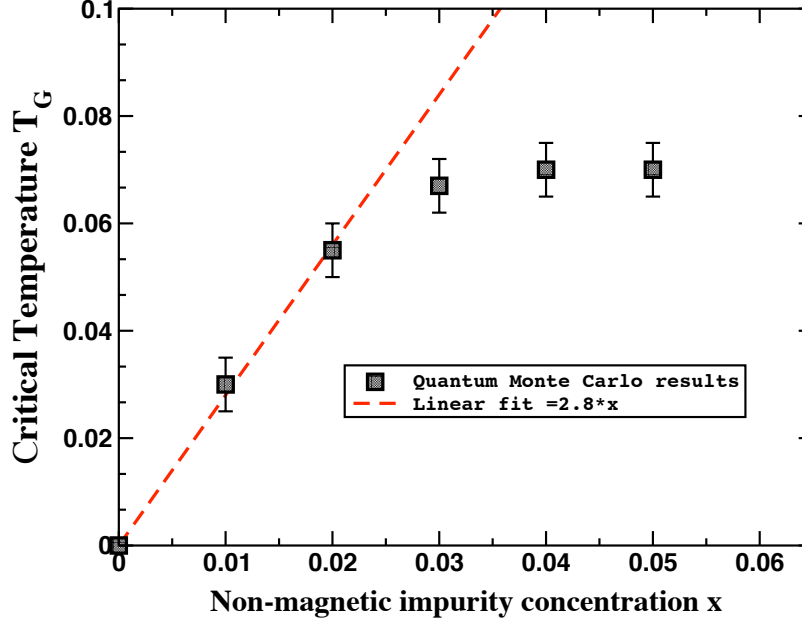


FIG. 2: (Color online) Critical temperature T_G (in units of J) plotted versus impurity concentration x .

between the two regimes, there is a well-known finite size scaling

$$\rho_s(L) \sim L^{2-D-z}, \quad (3)$$

where D is the space dimension (here $D = 3$) and z is the dynamical exponent ($z = 0$ for a finite temperature phase transition). Therefore we expect $\rho_s \times L$ to be a constant at the critical point where a crossing of the various system sizes should occur. We thus used such a criterion to identify the ordering transition at $x = 1, 2, 3, 4, 5\%$. Results of such an analysis for a concentration $x = 2\%$ are displayed in Fig. 3 for $L = 16, 24, 32, 48$ with a critical point found at $T_g = 0.055J$. In Fig. 3(A), we show the average stiffness versus T/J . In fact the spin stiffness is a directionnal quantity and can thus be computed in all space directions x, y, z , or averaged over all directions. The crossing of $\rho_s \times L$ is shown in Fig. 3(B) as well as in insets (X,Y,Z) for all the components of the stiffness. This clearly shows that the ordering is fully three dimensional and we find a remarkable agreement for the crossing temperatures in all directions at $T_g/J = 0.055$.

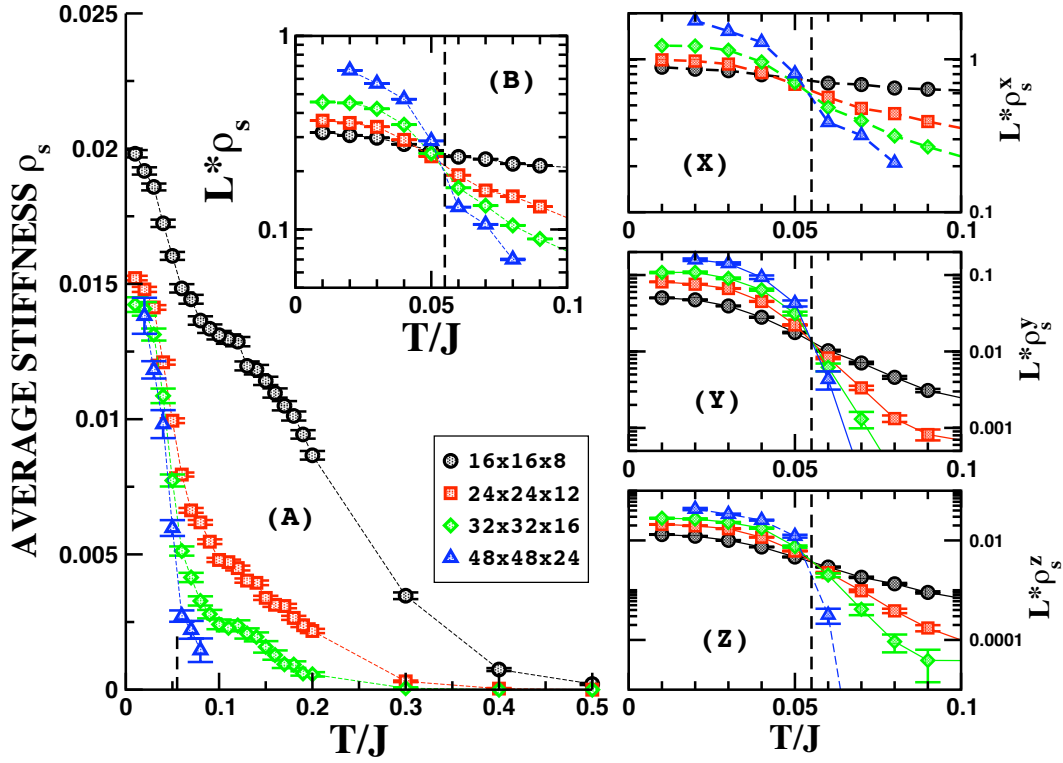


FIG. 3: (Color online) QMC results for the 3D model of coupled ladders with $x = 2\%$ of non-magnetic impurities. (A) shows the average 3D stiffness versus T/J . The same data are shown in (B) where $\rho_s \times L$ has a crossing for all sizes at $T/J = 0.055$. Insets (X,Y,Z) show all the components of the spin stiffness times L that cross at the same critical temperature.

V. COMPARISON TO EXPERIMENTS AND CONCLUSIONS

To finally conclude on this issue of the 3D transition, we carefully checked that the ordering transition is a true AF 3D ordering which occurs at a freezing temperature T_g proportionnal to the average coupling as proposed in the paper [1]. We indeed confirm a linear regime with x at low concentration followed by a saturation a larger x corresponding to the fact that the average distance between impurity start to be of the order of the correlation length ξ . As a comparison we plotted on a common graph (Fig. 4) experimental results for T_g rescaled to their $x = 3\%$ values for various spin-gapped materials together with the QMC results of this study. The agreement is very good.

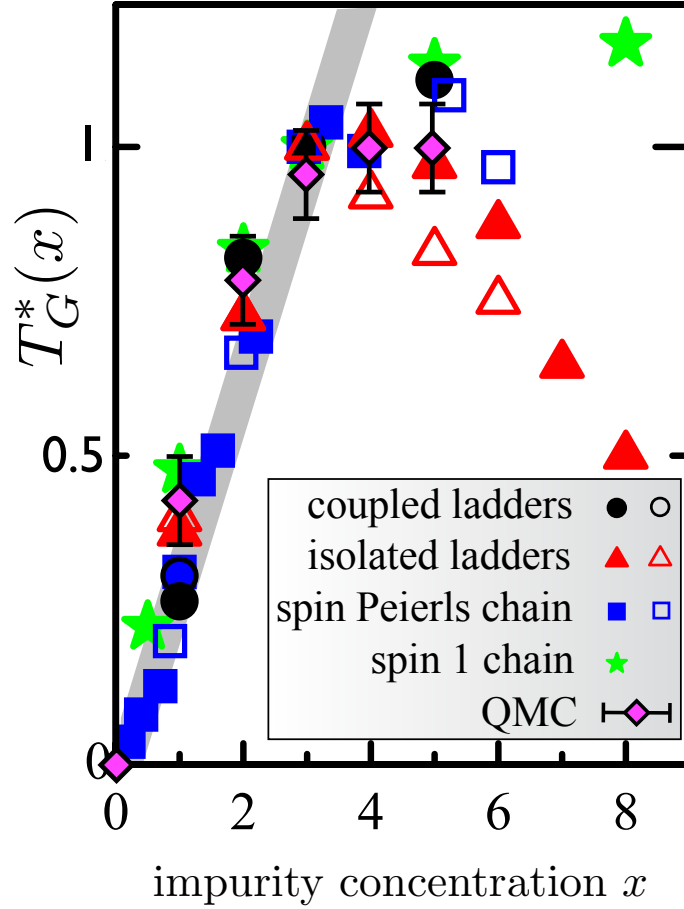


FIG. 4: (Color online) Transition temperatures T_g^* (rescaled to their values at $x=3\%$) versus impurity concentration for various low-D spin-gapped systems: coupled ladders $\text{Bi}(\text{Cu}_{1-x}(\text{Zn or Ni})_x)_2\text{PO}_6$ from this study; isolated ladder $\text{Sr}(\text{Cu}_{1-x}(\text{Zn or Ni})_x)_2\text{O}_3$; Haldane chain $\text{Pb}(\text{Ni}_{1-x}\text{Mg}_x)_2\text{V}_2\text{O}_8$; spin-Peierls chains $\text{Cu}_{1-x}(\text{Zn or Ni})_x\text{GeO}_3$. QMC data of Fig. 2 are also shown for comparison.

-
- [1] J. Bobroff, N. Laflorencie, L. K. Alexander, A. V. Mahajan, B. Koteswararao, and P. Mendels, *Phys. Rev. Lett.* **103**, 047201 (2009).
 - [2] M. Sigrist and A. Furusaki, *J. Phys. Soc. Jpn.* **65**, 2385 (1996).
 - [3] M. Imada and Y. Iino, *J. Phys. Soc. Jpn.* **66**, 568 (1997).
 - [4] C. Yasuda *et al.*, *Phys. Rev. B* **64**, 092405 (2001).
 - [5] N. Laflorencie and D. Poilblanc, *Phys. Rev. Lett.* **90**, 157202 (2003).
 - [6] S. Wessel *et al.*, *Phys. Rev. Lett.* **86**, 1086 (2001).
 - [7] H. Weber and M. Vojta, *Eur. Phys. J. B* **53**, 185 (2006).
 - [8] A. W. Sandvik, *Phys. Rev. Lett.* **80**, 5196 (1998).